Impact of sulfonated poly(ether ether ketone) membranes pretreatments on their physicochemical properties and fuel cell performances

Meriem Daoudi, Evelise Ferri, Claire Tougne, Assma El Kaddouri, Jean-christophe Perrin, Jérôme Dillet, Laurent Gonon, Vincent Mareau, Hakima Mendil-jakani, Veronique Dufaud, et al.

Impact of Sulfonated Poly(Ether Ether Ketone) Membranes Pretreatments on their Physicochemical Properties and Fuel Cell Performances

Meriem Daoudi [1], Evelise Ferri [2,3], Claire Tougne [4], Assma El Kaddouri [*1], Jean-Christophe Perrin [1], Jérôme Dillet [1], Laurent Gonon [4], Vincent Mareau [4], Hakima Mendil-Jakani [4], Veronique Dufaud [2], Eliane Espuche [3], Olivier Lottin [1]

[1] *Université de Lorraine, CNRS, LEMTA, 54000 Nancy/France*

[2] *Univ. Claude Bernard Lyon 1, CNRS, CP2M, 69001 Lyon/France*

[3] *Univ. Claude Bernard Lyon 1, CNRS, IMP, 69001 Lyon/France*

[4] *Univ. Grenoble Alpes, CEA, CNRS, Grenoble SyMMES, 38000 Grenoble/France*

** Corresponding author: assma.el-kaddouri@univ-lorraine.fr*

Journal of Polymer Science, **2023, 61(9), pp. 761–776 - https://doi.org/10.1002/pol.20220649**

Abstract

This work focuses on the impact of sulfonated Poly(Ether Ether Ketone) (sPEEK) membrane pretreatments on fuel cell performance, starting from two different batches of Fumapem E730 from Fumatech, acquired in 2019 and in 2020. sPEEK membranes are possible lower cost alternatives to PerFluoroSulfonic Acid (PFSA) membranes for Proton Exchange Membrane Fuel Cells (PEMFC) applications. Before use, they must be pretreated to ensure a complete protonic substitution and removal of residual reagents/solvent: the simplest protocol consists in soaking the membrane in an acid solution followed by a rinsing step in water. In addition to this acidification step, hydrothermal (*HT*) treatments in water at high temperature for a few hours to a few days were also considered herein, as well as a hydro-alcoholic (*HA*) step, because of their expected effects on membrane nanostructure. Overall, four different protocols were used. The membrane water uptake, water self-diffusion, proton conductivity, and fuel cell performance -under H_2/O_2- were measured. It was found that in the best case -membranes from the 2020 batch subjected to *HA* followed by 72 hours *HT* pretreatments- the fuel cell performances exceeded those obtained with a PFSA membrane (Nafion XL). This is explained by a higher protonic conductivity, probably resulting from a better sPEEK nano-structuration.

Keywords: PEMFC, sulfonated poly(ether ether ketone) membrane, pretreatment, performance

Funding: This work was partially supported by the French National Research Agency (project ANR-18-CE05-0027 MULTISTABLE).

1. Introduction

Proton exchange membrane fuel cells (PEMFC) are promising clean energy-delivery devices, especially for automotive and stationary power applications, with much less pollutant emissions than their current counterparts like internal combustion engines[1,2]. The heart of a PEMFC is the membrane electrode assembly (MEA), where the electrochemical reactions take place. It is made of two gas diffusion layers (GDL), and two dispersed catalyst layers separated by the proton exchange membrane used as electrolyte[3].

The most common membranes used in PEMFC are thin films of perfluorosulfonic acid copolymers (PFSA) such as Nafion®, with a proton conductivity approaching 0.1 S cm^{-1} in ideal conditions, a good chemical stability, and fast hydration dynamics[4,5]. These remarkable properties stem from both the superacidity of the ionic functions and their unique microstructure[6,7]. However, the high cost of PFSA, their loss of conductivity at low humidity and consequently at high temperature (>80°C), make their use complex and limit their application range[8,9]. Therefore, many works have been devoted to the development of lower cost hydrocarbon (HC) alternatives to PFSA. Among them, sulfonated poly(ether-ether-ketone) (sPEEK) membrane are cheap, offer good mechanical properties and a high proton conductivity: from 2.2×10^{-2} S cm^{-1} to 1.1×10^{-1} S cm^{-1} for a degree of sulfonation varying between 0.69 and 0.96 according to Kaliaguine *et al* and Do *et al*[10,11]. In addition, sPEEK membranes have shown good performances in hydrogen fuel cells on several occasions[12–15] although they still suffer from insufficient durability because of their high sensitivity to radical attacks[16].

However, the cell performance of MEA made with sPEEK membrane depends not only on the properties of the raw material but also on:

- the membrane pre-treatment, directly impacting its microstructure and thus its proton conductivity, and performances[17–19] ;
- the quality of the interface between the membrane and the electrode, in terms of proton transfer or ionic resistance, *i.e.* the way the MEA are actually assembled or made (spray coating, hot pressing, …). This point is an issue with sPEEK membrane because of the difference between their chemical structure and properties and those of the PFSA used in the electrodes. For example the glass transition temperature of the sPEEK is in the range of 170-220°C [20,21] while it is only about 120°C [22] in the case of PFSA.

sPEEK membranes must be pretreated before use to ensure a complete protonic substitution and removal of residual reagents/solvent[9]. This is generally done by soaking the sample in an acid solution, either at room temperature or at high temperature, usually 80°C[9,14,23–25]. Mun-Suk Jun *et al*[9] showed for instance that soaking sPEEK membranes prepared by

different casting solvent in 1M sulfuric acid for 12 hours at 80°C improved their proton conductivity and cell performances compared to non-pretreated membranes.

In addition to these activation or cleaning steps, many works[13,17,18,26–29] have highlighted the interest of a supplementary hydrothermal treatment in water at high temperature for a few hours to a few days to improve the microstructure of the membrane -by increasing the connectivity and swelling of the hydrophilic domains- with expected positive effects on performances. For instance, Mendil-Jakani *et al.*[18] studied the impact of the time-temperature relationship of an additional hydrothermal treatment on the structure and properties of Fumapem® sPEEK membranes purchased from Fumatech®. They concluded that soaking the membrane 72 hours in water at 80°C led to an excellent hydrophilic/hydrophobic nanophase separation and therefore an improved proton conductivity. This hydrothermal transition was attributed to the glass transition crossover T_β of the polymer backbone[18]. In water, relatively long treatments were necessary to obtain well-defined ionic channels at temperatures close to T_β (much shorter durations when $T >> T_\beta$). In order to reduce the temperature and the duration of the treatments, polar solvents such as alcohol, known to induce strong swelling[30,31] (mass and volume) of ionomer membranes (solvation of ionic sites and solvent plasticizing effect) were used to increase the macromolecular mobility.

Herein, we studied the impact of various sPEEK membrane pretreatments on membrane properties and fuel cell performances using two different batches of Fumapem E730 from Fumatech, acquired in 2019 and in 2020. Four different protocols were tested. The first consists only in membrane acidification and rinsing, while the three others also include a hydrothermal treatment in water at 80°C, from 1 hour to 72 hours, and possibly an additional hydro-alcoholic treatment. Then, the proton conductivity, water self-diffusion and sorption properties of the membrane were evaluated; the samples were also used to make Membrane Electrodes Assemblies to assess their functional properties in a 7.22 cm^2 (1.9 cm x 3.8 cm) cell. We compared the polarization curves obtained with the different MEA, performed cyclic voltammetry to assess the electrodes ElectroChemical Surface Area (ECSA), and measured the hydrogen permeation current as well as impedance parameters such as the high frequency resistance.

2. Materials and methods

2.1. Electrochemical characterizations

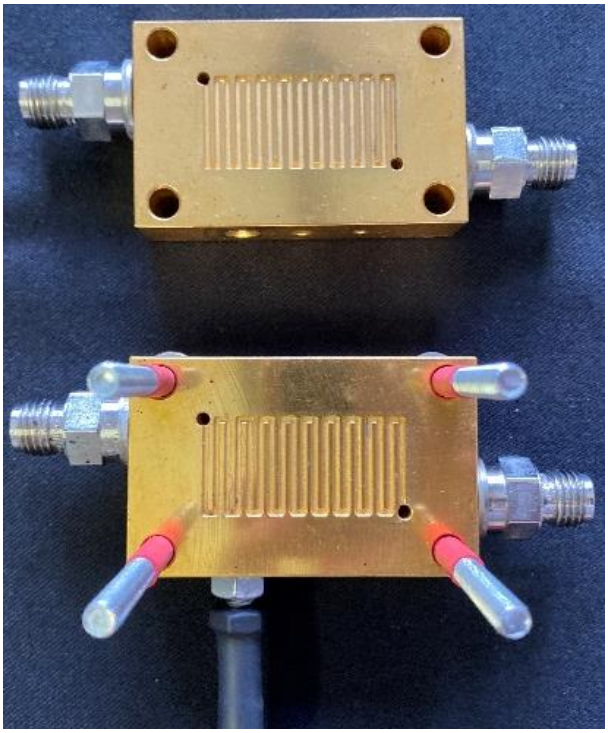

Figure 1. Single cell with two identical flow field plates used to test the MEA.

The MEA performance was tested in a single cell made of two identical gold-coated stainless steel plates on the anode and cathode sides, with single serpentine channel (19 passes) of 0.7 mm in depth and 1 mm in width (**Figure 1**). The cell was operated at atmospheric pressure and fed in counter-flow with 80% Relative Humidity (RH) hydrogen and oxygen (unless otherwise stated). The gas stoichiometries were set to 1.5 on both sides. The flow field plate temperature was controlled thanks to a water circulation loop and set to 70°C in usual conditions. To avoid any damage to the MEA during the start-up procedure, the temperature was slowly increased from 40°C to 70°C for 40 minutes while both the anode and cathode compartments were flushed with 10 slph (standard liters per hour) of 60% RH nitrogen.

Each new MEA was subjected to a four-hour break-in stage, consisting in the repetition of potentiostatic steps at OCV (30 s), 0.6 V (45 s) and 0.3 V (60 s). The FC was then operated for two hours at a constant current density of 0.5 A/cm² to make sure the MEA performance was stable. The MEA were eventually fully characterized using the following protocol:

- **Electrochemical Impedance Spectroscopy (EIS):** the impedance spectra were measured at 0.5 A/cm^2 in galvanostatic mode with a frequency ranging from 0.02 Hz to 10 kHz with a perturbation amplitude of +/- 5 % (+/- 25 mA/cm²). In this work EIS was used mostly to assess the FC high frequency resistance R_{hf}.
- The **polarization curves** were measured between 1 V and 0.4 Vby increasing and then decreasing the current density. It was varied by steps of 50 seconds from 0.03 A/cm² (at low current density) to 0.15 A/cm² (at high current density). Figures 3 and 4 in the result section show the average cell voltage while the error bar is the difference between the values obtained by decreasing and increasing the current density.
- The **Hydrogen permeation currents** were measured by flushing the cathode compartment with 10 slph of nitrogen, while the anode compartment was flushed with 10 slph of hydrogen. The hydrogen permeation currents were then estimated by subtracting the average values measured at 0.6 V -during 120 seconds- from those measured at OCV. Hydrogen permeation currents were used to detect faulty membranes, as their raw value is quite difficult to interpret [32] without varying the measurement parameters.
- The **Electrochemical surface area (ECSA**) was measured under nitrogen (0 slph) in the cathode compartment and hydrogen (10 slph) in the anode compartment by sweeping the potential from 0.1 V to 0.7 V with a scan rate of 50 mV/s.

This characterization sequence was repeated three or five times with 80 % RH gases to check for the stability of performances. For simplicity only the lastest data are presented here. In addition, the tests were always repeated after switching the oxygen and hydrogen flows, i.e. after reversing the anode and the cathode, to verify the repeatability and homogeneity of the MEA assembly process.

Note that the whole characterization sequence was in some cases also performed with 60% RH gases. Nevertheless, the performances being most of the time slightly lower, except at low current density, the results obtained at low RH are not presented in this paper.

2.2. Preparation of membrane electrodes assemblies

A preliminary step in fuel cell performances testing was to achieve a good adhesion between the sPEEK membrane and the electrodes to make a functional MEA: although the performance of PEMFC depends mainly on the membrane and the electrodes, the interfacial electrical resistance between them must also be as low as possible. This point is generally not an issue in the case of PFSA membranes because this ionomer is also used as an electrode component to ensure ionic conductivity (through the electrodes). However, two difficulties may be encountered when using sPEEK membranes: (i) poor adhesion with the electrodes when gas

diffusion electrodes (GDE) or catalyst coated backing (CCB) are used and/or (ii) significant interfacial resistance between the membrane and the electrodes, even when a good adhesion is reached.

Several strategies were tested in the literature to enhance the sPEEK membrane/electrodes interface[33–43]. For instance, some groups considered using hydrocarbon-based ionomers as binder materials in the catalyst layers (CL)[34,35]. However, they concluded that even though this strategy enhances the interfacial contact between the membrane and the catalyst layers (CL), the low proton activity and oxygen permeability of hydrocarbon (HC) ionomer resulted in poor performances, [44,45]. Therefore, despite the low affinity between sPEEK and PFSA leading to a poor interfacial adhesion, the use of PFSA in the catalyst layer with an sPEEK membrane remains inevitable[41].

Other groups considered adding PFSA to a hydrocarbon membrane to improve the cohesion with the CL. For instance, Jung et al.[36] prepared sPEEK/poly(vinylidene fluoride) (PVdF) blend membrane, to improve -*vs*. sPEEK membranes- its dimensional stability and its chemical compatibility with electrodes containing Nafion®. They found that the MEA made with such hybrid membranes had stable performances for around 1650 hours when a small amount of PVdF (2.5 wt%) was incorporated. Moreover, Wiles et al. [37] reported that the partial fluorination of poly(arylene ether sulfone) membrane improves the adhesion with Nafion®-bonded electrode by decreasing the high frequency resistance.

In several other works, the authors considered adding bonding layers to reinforce the adhesion between the membrane and the electrodes[33]. For example, Choo et al[38] used a cross-linked interfacial layer containing sulfonated poly(ether ether ketone) (sPEEK) and Nafion®. They found that the interfacial layer improved the compatibility between the CL and the membrane, as well as its dimensional stability. As a result, the long-term stability of performances was significantly improved after wet-dry cycling test. A significant enhancement of the interfacial adhesion between HC SPAES (poly(arylene ether sulfone)) membranes and Nafion® -based CL was also obtained by spraying a thin bonding layer made of SPAES (poly(arylene-ether-sulfone)) and PVdF on the membrane surface[39]. Alternatively, Nam et al.[40] used a sulfonated aromatic copolymer with flexible and partially fluorinated structures as a bonding layer to enhance the adhesion between SPAES and Nafion®-based CL. And they recently presented a new approach based on the creation of an interfacial bonding layer between SPAES membrane and PFSA-based CL with a composition gradient: three sublayers containing SPAES and PFSA ionomer with different weigh ratios were sprayed on the membrane[41]. Finally, Oh et al.[42] developed a strategy based on physical interlocking without chemical treatment, in which micrometer-sized pillars were formed on the SPAES

surface and intruded into Nafion®-based CL. They obtained a better durability of the MEA under wet/dry cycles.

Herein we added a Nafion® overcoat as an interfacial bonding layer on commercial GDE (gas diffusion electrodes: 220 µm thick Sigracet 29BC, with 0.3 mg_{Pt}/cm^2, and 40% platinum on Vulcan carbon) to enhance the interfacial contact between sPEEK membrane and electrode. Different thickness of Nafion® overcoat were tested, from 9 mg/cm² to 0.25 mg/cm² (*i*.e. 45.4 µm to 1.26 µm assuming a Nafion® dry density of 1980 kg/m^3 [46]). A first attempt showed that a good adhesion could be reached, but at the expense of the cell performances when the Nafion® overcoat increased from 0.4 mg/cm² to 9 mg/cm² (2.02 µm to 9.09 µm). In a second step, the thickness of Nafion® was optimized, using two of the thinnest overcoats we could achieve with a spraying machine (ExactaCoat Sono-Tek coating system with ultrasonic nozzles): 0.25 mg/cm² and 0.5 mg/cm² (1.26 µm, 2.53 µm). In addition, Sigracet 29 BC GDE were also purchased from an external manufacturer with an additional 0.3 mg/cm² Nafion® overcoat (**Table 1**).

All these preliminary tests were performed using Fumapem® E730 membranes from Fumatech®, acquired in 2020 pretreated according to the protocol recommended by the manufacturer (see section 2.3).

Table 1. Nafion® overcoat on 220 µm thick Sigracet 29BC GDE.

	Home-made		Purchased
Nafion® weight (mg cm^{-2})	0.25	0.5	0.3
Estimated thickness (µm)	1.26	2.53	1.52

Starting from the Nafion coated GDE in **Table 1**, the MEA were made following a protocol close to that described by Robert et al.[47]:

- 70×45 mm^2 membranes were inserted between two 18×37 mm^2, 23 µm thick, polyethylene terephthalate (PET) reinforcement sheets to enhance the stiffness of the assembly and to avoid direct contact with gases during operation.
- Two identical Nafion®-coated GDE were then placed on both sides of the membrane and held in place using 100 µm polytetrafluoroethylene (PTFE) seals (**Figure 2**).
- The assembly was then placed between two aluminum plates covered with PTFE and slightly pressed (~ 50 N) for 8 minutes, i.e. the time needed to reach a uniform temperature of 135 °C throughout the plates and MEA.
- Finally, the MEA were hot pressed at 135°C for 3 minutes 30 seconds at 4600 N.

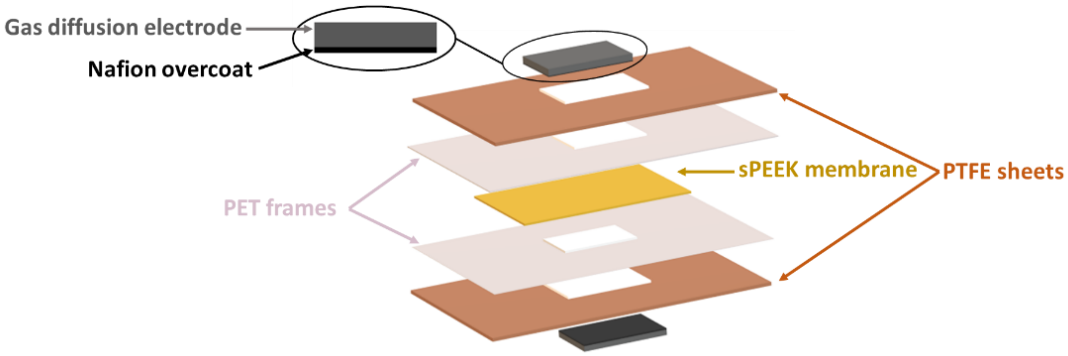

Figure 2. Illustration of the MEA fabrication process.

MEA were also made using Nafion XL membrane for comparison purpose (see section 3.3.). In this case, GDE was used with and without overcoat to evaluate its impact on FC performance, and the applied pressure was slightly lower (3000 N) due to the lower glass transition temperature of PFSA [48].

2.3. Membrane pretreatments

To study the influence of hydrothermal and hydro alcoholic pretreatments on fuel cell performances, four different protocols were applied on two different batches of Fumapem® E730 membrane (28 to 33 µm thick and with an IEC of 1.29 meq g^{-1} according to the manufacturer – see also the results in section 3.1) from Fumatech®, purchased in H-form. In the following, the first batch is labelled -sPEEK 2019- and the second one is labelled -sPEEK 2020-. The first batch was purchased initially to carry out studies related to the chemical stabilization of sPEEK membranes (reference [13], and another work that will be published shortly). The second batch was purchased to perform some reproducibility tests, but it quickly appears that there were some significant differences between these two batches, although they were presented as identical by the manufacturer: although the chemical formulation of the ionomer is unchanged, Fumapem may have change the fabrication process and/or solvent they used, which translated into different properties and behavior. We will return to this point later in the paper.

First pretreatment: *acidification and rinsing*.

This first pretreatment protocol consists in soaking the membrane in a 1M sulfuric acid solution for 4 hours at 80°C,. The samples are then rinsed three times with deionized water for 15-20 minutes and dried in an oven at 100 °C for 18 hours. This protocol is the most commonly used in the literature to remove the impurities and the remaining solvent[49,50]. The membranes undergoing this protocol are referred to as *sPEEK 2019 Acd* and *sPEEK 2020 Acd* in the following.

Second pretreatment: *acidification-hydrothermal 1 hour*.

The second pretreatment protocol consists in soaking the membrane first in a 1M sulfuric acid solution for 16 hours at 80°C, then in water for one hour at 80°C. The samples are then rinsed three times with deionized water for 15-20 minutes and dried in an oven at 100 °C for 18 hours. This protocol is recommended by Fumapem®. The membranes undergoing this protocol are referred to as *sPEEK 2019 Acd-HT 1h* and *sPEEK 2020 Acd-HT 1h* in the following.

Third pretreatment: *acidification-hydrothermal 72 hours-acidification*.

The third pretreatment protocol consists in soaking the membrane in 1M hydrochloric acid solution at room temperature for 4 hours, rinsing three times with deionized water for 15-20 minutes, and soaking in water for 72 hours at 80°C. After that, the samples have to be reacidified in a 1M hydrochloric acid solution at room temperature for 4 hours. Finally, the membranes are rinsed again, as described above, and dried under dry air at room temperature for 72 hours. This protocol was proposed by Mendil-Jakani *et al.*[18] to improve the ionomer nanophase separation. However, it could be applied only to the 2019 batch (*sPEEK 2019 Acd-HT 72h-Acd*) since membranes from the 2020 batch do not withstand the hydrothermal treatment right after the acidification step: they swelled up too much and became very difficult to handle.

Fourth pretreatment: *acidification-hydro alcoholic-hydrothermal 72 hours*.

A fourth protocol was tested to enhance the nanophase separation of the 2020 sPEEK membranes without excessive swelling. It consisted in inducing the swelling[30,31] through a hydro alcoholic step in water/ethanol solution (64/36 vol%) before the hydrothermal treatment (80°C/72h). This protocol was also applied for comparison to the 2019 batch. These membranes were labeled *sPEEK 2020 Acd-HA-HT 72h* for the batch 2020 *and sPEEK 2019 Acd-HA-HT 72h* for the batch 2019*.*

2.4. Sorption isotherms

A dynamic vapor sorption (DVS) analyzer (IGAsorp, Hiden Isochema) with a mass resolution of about ± 0.2 µg was used to measure the membranes sorption isotherms. The samples were first dried for 5 hours at 100°C under a nitrogen flow rate of 250 mL.min^{-1} to determine their dry mass. Then, sorption isotherms were recorded at 30°C ± 0.1°C, the relative humidity (RH) varying between 0% and 95% with an increment of 5 or 10%. The DVS analyzer technique to assess the sample equilibrium mass consists in fitting in real time the weight relaxation curve using a standard model based on Fick's diffusion[51]:

$$m(t) = m_0 + [m_\infty - m_0]\left[1 - e^{-kt}\right]$$

With m_0, the initial weight of the sample, t the elapsed time since the last RH step, and m_∞ the (assumed) sample equilibrium weight. The equilibrium threshold was fixed to $0.99 \times m_\infty$ and the maximum time devoted to each RH step was set to 10 or 40 hours depending on the experiment (see the discussion in section 3.5): in other words, a new RH step was started once the membrane mass had stabilized, so that $\frac{m(t)}{m_\infty} \geq 99\%$, or after 10 or 40 hours when that value was not reached.

2.5. Water self-diffusion coefficient

The in-plane water self-diffusion coefficient was measured by liquid-state ^{1}H-NMR spectroscopy using a Pulsed-Gradient STimulated spin-Echo (PGSTE) sequence with unipolar magnetic field gradients. The spectra were acquired at 600.13 MHz on a Bruker Avance III WB spectrometer using a 5 mm Diff30 probe delivering a maximum gradient intensity of 1800 G.cm^{-1}. The measurements were carried out at 24°C, with a gradient pulse duration $\delta = [0.66 - 2.00]$ ms, a diffusion delay $\Delta = [3.8 - 13.0]$ ms and a gradient strength g between 40 and 1000 $G.cm^{-1}$. 256 scans were recorded and averaged using a recycle delay of 3 s. The water self-diffusion coefficient was then determined by fitting the signal attenuation as a function of the gradient strength with the Stejskal – Tanner equation[52]. Water self-diffusion coefficient of 2 x 4 cm² samples was measured for different water contents: some samples were fully immersed in distilled water at room temperature for several hours while others were directly analyzed in dry state, depending on the measurements campaign. In the case of immersed membranes, the hydrated samples were immediately pressed between two layers of absorbent paper once out of water to remove residual droplets, before being rolled and packed into 5 mm airtight NMR tubes. In both cases, the samples were equilibrated at least overnight before being weighted and analyzed. The hydration level of each sample was then adjusted by exposing them to a water-saturated environment or to the ambient atmosphere to increase or decrease the water content, as needed. No discrepancy was observed in the evolution of the water self-diffusion coefficient as a function of the water content between the two operating modes, *i.e.* whether the membrane samples were first hydrated and then dehydrated, or the other way.

2.6. Proton conductivity

The in-plane resistance was measured by voltammetry by performing a linear voltage sweep using an Essential VSP Potentiostat (BioLogic Science Instrument) and a BT-110 conductivity clamp (four-electrode method,31 Scribner Inc., USA) at room temperature. Membranes were rehydrated by an immersion in water for 72 hours then re-acidified in a 1 M HCl solution at room temperature for 4 hours, triple rinsed with pure water before measurements. The slope

of voltage vs. current response was used to calculate the resistance (R in Ω), and the in-plane conductivity σ (S.cm^{-1}) was calculated according to:

$$\sigma = \frac{L}{WeR}$$

with L the distance between the inner V-sense electrodes (cm), W the membrane width (cm) and e the membrane thickness (cm).

3. Results

3.1. Membrane thickness

After each pretreatment, the thicknesses of all membranes were measured at ambient humidity and temperature using a digital micrometer with a precision of ± 1 µm. For each sample, the thickness was measured on six to eight different areas to account for possible heterogeneities and this protocol was repeated with two to four samples per batch and pretreatment, including as-received membranes. **Table 2** shows that the pretreatments result in a small thickness decrease of about five micrometers compared to as received membranes. This was observed in all cases, except with samples from the 2020 batch subjected to the acidification-hydro alcoholic-hydrothermal 72 hours pretreatment (sPEEK 2020 Acd-HA-HT 72h), which underwent a much more significant thinning of 47%, yielding a 16.7±3.2 µm membrane thickness. The thinning of this membrane was accompanied by an increase of its in-plane dimensions of 21±13%, while no significant change was observed with the other pretreatments. Note that the thickness, length and width were always measured after drying the samples (18 hours at 100°C).

Table 2. Membrane thickness before pretreatment (as received) and after pretreatment (at the dry state).

Membrane	Thickness (µm)
sPEEK 2020 As Received	31.7 ± 0.9
sPEEK 2019 As Received	29.5 ± 1.2
sPEEK 2020 Acd	26.8 ± 1.3
sPEEK 2020 Acd-HT 1h	25.5 ± 1.7
sPEEK 2020 Acd-HA-HT 72h	16.7 ± 3.2
sPEEK 2019 Acd	27.9 ± 1.0
sPEEK 2019 Acd-HT 1h	26.9 ± 1.0
sPEEK 2019 Acd-HA-HT 72h	28.1 ± 0.5
sPEEK 2019 Acd-HT 72h-Acd	24.1 ± 1.1

3.2. Optimization of Nafion overcoat

Figure 3 shows the polarization curves measured with 2020 Fumapem E730 sPEEK membranes subjected to the activation protocol recommended by the manufacturer (Acd-HT 1h, *i.e* second pretreatment in section 2.3.) and assembled with GDE with Nafion® overcoat as described in Table 1. The highest performances were obtained with the two thinnest Nafion® overcoat: 0.25 mg/cm^2 and 0.3 mg/cm^2.Their polarization curves are almost similar at low current density. , but the decrease of the voltage observed at high current density is greater with the home-made 0.25 mg/cm^2 Nafion® overcoat than with the 0.3 mg/cm^2 overcoat applied by the GDE supplier. These results are consistent with the values of the high frequency resistance R_{hf}, keeping in mind that its value results from the protonic resistance of the membrane, the ionic and electrical resistances of all FC components, as well as the interface resistances between them[53,54]. The R_{hf} measurements in **Table 3** show that the lowest value, R_{hf} = 70 ± 7 mΩ.cm², was obtained with the 0.3 mg/cm^2 overcoat applied by the GDE supplier. Such variations between the three overcoats can be attributed to both their thickness and their making processes: the Nafion layer was sprayed in the lab in the case of the 0.25 and 0.5 mg/cm^2 coatings and applied by the GDE supplier in the case of the 0.3 mg/cm^2 coating. In addition to the high frequency resistance, **Table 3** also shows the values of ECSA that were obtained with the three overcoats, *i.e*. the active surface area of the electrodes measured by adsorption/desorption of hydrogen on platinum on the cathode side[55–59]: the highest value (26.7 m^2/g) was also obtained with the 0.3 mg/cm^2 overcoat. The slightly lower ECSA found with the home-made 0.25 mg/cm^2 and 0.5 mg/cm^2 overcoat may be explained by a greater penetration of ionomer into the catalyst layer hindering gas diffusion through the catalyst layer[55].

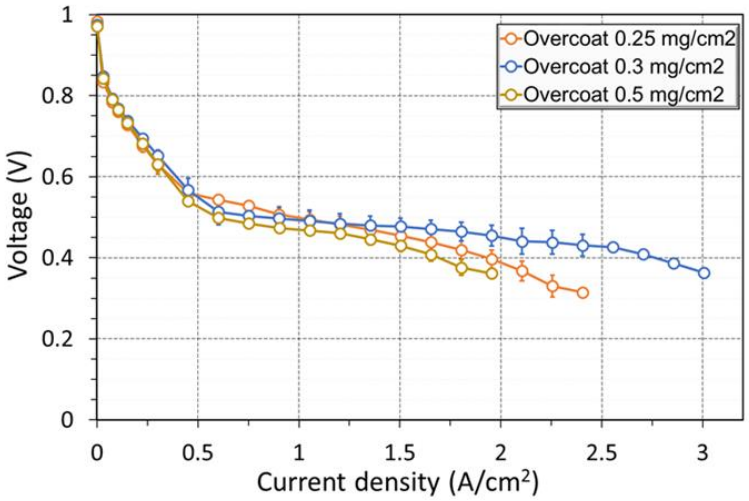

Figure 3. O_2/H_2 polarization curves of 2020 Fumapem E730 sPEEK membranes subjected to acidification and 1-hour hydrothermal pretreatments, as advised by Fumatech (see section **2.3**.). GDE and Nafion® overcoats described in **table 1.**

As a conclusion from this preliminary work, we have decided to retain the GDE with ionomer coating provided by the manufacturer (0.3 mg/cm^2) since they gave better and more repeatable performances. All the results presented in the following sections of this paper were thus obtained using these GDE, following the MEA making protocol described above. However, it must be kept in mind that performing a complete optimization of FC performances using such sPEEK membranes would have required to consider other MEA manufacturing techniques (spray coating, decal transfer… , with adapted ionomer content), possibly other choices of GDL, as well as a complete cartography of the operating conditions (gas RH, pressure and flow rates, FC temperature) and even other flow fields geometry. For obvious reasons, such a work was considered outside the scope of this study and the performance we achieved with this assembly protocol and test configuration should only be considered sufficient to analyze the impact of the different sPEEK pretreatments presented in the rest of the paper.

Table 3. High frequency resistance and surfaces actives area of MEA fabricated using gas diffusion electrodes with different Nafion® overcoat.

	Overcoat 0.25 mg/cm^2	**Overcoat 0.3 mg/cm^2**	**Overcoat 0.5 mg/cm^2**
R_{hf} at 0.5 A/cm^2 (mΩ.cm^2)	98 ± 5	70 ± 7	106 ± 8
ECSA (m^2/g)	23.6 ± 1.6	26.7 ± 1.8	23.7 ± 1

3.3. Fuel cell performances

Polarization curves

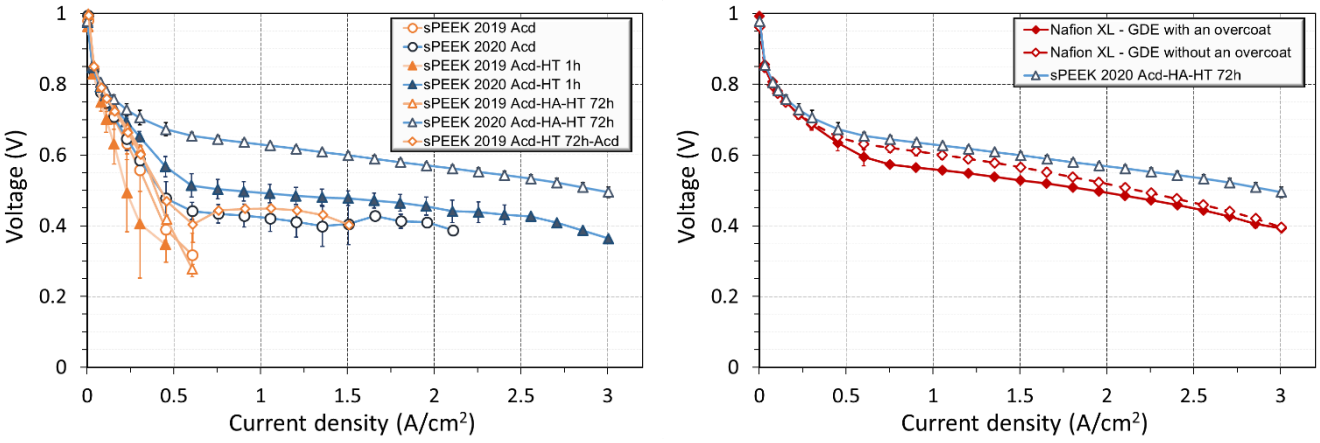

Figure 4. Left: O_2/H_2 polarization curves of 2019 and 2020 Fumapem E730 sPEEK membranes batches subjected to the four pretreatment protocols described in section 2.3. **Right:** comparison of the best performance obtained (*acidification-hydro alcoholic-hydrothermal 72 hours* with 2020 batch) with MEA assembled using Nafion XL membranes with and without Nafion overcoat on the GDE.

Figure 4 (left) shows O_2/H_2 polarization curves obtained with Fumapem E730 sPEEK membranes from 2019 and 2020 batches subjected to one of the four pretreatments described

in section 2.3. As mentioned in section 2.1, all MEA were broken-in following the same protocol, the gas stoichiometries were set to 1.5 on both sides, and the cell temperature to 70°C.

The polarization curves in **Figure 4** clearly show the very strong impact of the pretreatment protocols on the membrane performance when used in FC[60]. It must also be mentioned that in addition to being highly dependent on the membrane pretreatment the performances we measured were also reproducible as evidenced by the small error bars in **Figure 4**, especially at high current density. At least 2 MEA were tested in each case and, as mentioned in section 2.1, the measurements were also repeated after switching the oxygen and hydrogen flows. In other words, each electrode was used as an anode and as a cathode. Note that the highest dispersion that can be observed at low current density is, at least to some extent, attributed to instabilities in the FC operation, with presumably some liquid water accumulation in the gas channels due to the high inlet RH (80%) of hydrogen and oxygen: its value was kept deliberately high because this improved the FC performance at high current density. However, the high number of configurations tested did not allow to perform a thorough optimization of the performances as a function of the operating conditions.

Figure 4 also shows that when identical pretreatments were applied to the 2019 and 2020 batches (same symbols on the curves), FC performances were always better, or much better with the 2020 batch. However, it must be recalled that the 3rd protocol (acidification-hydrothermal 72 hours) could not be applied to the 2020 batch membranes because it made them fragile and very difficult to handle. In the absence of information provided by the manufacturer on the differences in the behavior of the 2019 and 2020 batches –they are identical according to their commercial description- we are currently unable to interpret with certainty their different behaviors. The difference can be tentatively explained by the impact of the casting solvent (different between 2019 and 2020) on the resulting self-assembling properties which is a well-reported phenomenon [50,61,62].

Finally, to emphasize the impact of pretreatments on FC performances, **Figure 4** (right) allows to compare the best sPEEK polarization curves (acidification-hydro alcoholic-hydrothermal 72 hours with E730 2020 batch) to those obtained using Nafion XL, a reinforced PFSA membranes of similar initial thickness (*i.e*. 27.5 µm [63,64], *vs*. 28-33 µm for Fumapem E730 according to the manufacturer) and in identical conditions. To consider a possible influence of the Nafion overcoat on the polarization curves (*via* for instance a different ionic series resistance and/or mass transfer limitation through the active layer), MEA made with Nafion XL were assembled with and without overcoat. In all cases, the polarization curve measured with the sPEEK membrane is higher than those obtained with Nafion XL. One can also see that the

PFSA overcoat has a slight impact on the FC voltage between 0.5 and 2.0 A/cm², *i.e*. 0.65 V to 0.5 V.

High frequency resistance and membrane conductivity

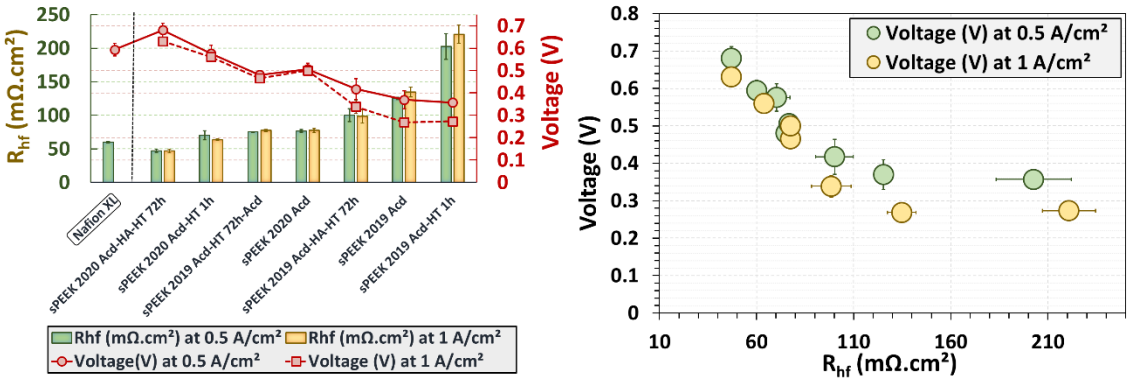

Figure 5. Left: high frequency resistance and FC voltage at 0.5 and 1.0 A.cm^{-2} vs. sPEEK pretreatments. Values obtained with Nafion XL are shown for comparison. **Right:** FC voltage at 0.5 and 1.0 A.cm^{-2} vs. high frequency resistance.

A complete understanding of the FC performance achieved with sPEEK membranes, as well as the differences between the various sPEEK pretreatments, will require a full electrochemical impedance spectroscopy (EIS) study to monitor key impedance parameters as a function of operating conditions. Nevertheless, it is worth reminding that the GDE were identical, so that the key factors governing variations in FC performance between all tested MEA are most likely the membrane conductivity and/or the quality of the membrane-electrodes interface, i.e. possible variations in the ionic interfacial resistance between sPEEK (in the membrane) and PFSA (in the electrodes) ionomers. Both the membrane conductivity and the membrane-electrodes interface resistance impact directly the FC high frequency resistance R_{hf}, and in turn, the FC voltage. Indeed, **Figure 5** (left) shows FC voltages and high frequency resistances, measured at 0.5 and 1.0 A.cm^{-2} (see section 2.1) as a function of the various sPEEK pretreatments. Values obtained with Nafion XL membranes are also shown for comparison. As expected, the membrane pretreatments giving the best performances are also those with the lowest high frequency resistance. Therefore, one can observe a very good correlation between the FC voltage and R_{hf}, as shown in **Figure 5** (right). It can be noted however that this correlation is less marked for the highest values of R_{hf} (i.e. in the two worst cases: acidification and rinsing, and acidification-hydrothermal 1 hour, both with the 2019 membrane batch), probably because the high frequency resistance is not the only impedance parameter governing the FC performance in these cases: a low quality interface between the electrodes and the membrane may for instance result in a higher charge transfer resistance if the operation of the electrode becomes more heterogeneous.

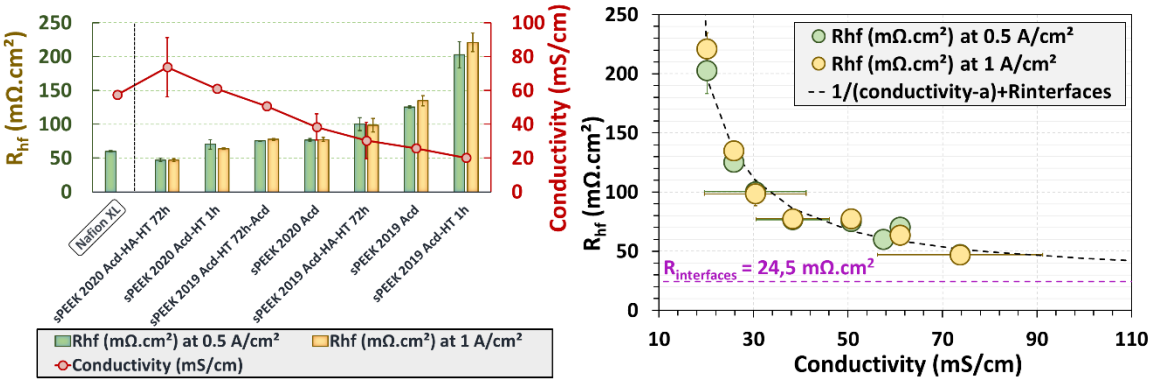

Figure 6. Left: high frequency resistance and membrane conductivity at room temperature vs. sPEEK pretreatments. Values obtained with Nafion XL are shown for comparison. **Right:** high frequency resistance vs. membrane conductivity.

Therefore, to distinguish the roles played by membrane conductivity and membrane-electrodes interfacial resistances, **Figure 6** (left) shows FC high frequency resistances -again at 0.5 and 1.0 A.cm^{-2}- together with the proton conductivity of the various membrane tested (see section 2.6) for the different pretreatments applied. As it could be expected, the lowest values of membrane conductivity correspond to the highest high frequency resistances and thus to the lowest FC voltage. **Figure 6** (right) also shows a good correlation between R_{hf} (vertical axis) and membrane conductivity (horizontal axis), although the membrane conductivity was measured in conditions (i.e. at room temperature, after soaking the samples in liquid water) that were not fully representative of FC operating conditions (i.e. 70°C and 80% RH inlet gases). One can thus conclude that the membrane conductivity is the main factor governing the observed variations in the FC high frequency resistance.

In a simplified approach in which the membrane ionic resistance is neglected when the ionic conductivity becomes very large, the high frequency resistance can be approximated as:

$$\mathrm{R_{hf}} = \mathrm{R_{membrane}} + \mathrm{R_{interfaces}} \sim \frac{1}{\mathrm{conductivity} - \mathrm{a}} + \mathrm{R_{interfaces}}$$

where a is a constant.

According to this formula, and the data of **Figure 6** (right), $\mathrm{R_{interfaces}} \sim 25\ \mathrm{m\Omega.cm^2}$ so that the interfacial resistance is responsible for about half of the total ionic resistance in the membranes that present the higher conductivity. A full characterization study of membrane conductivity would eventually be needed to better interpret these results, such as the work done by Maldonado *et al.* with Nafion[4].

3.4. Water self-diffusion coefficient

Mass transport in ionomer membrane plays a fundamental role during fuel cell operation. Transport phenomena through ionomer membrane include proton transport, as well as water self-diffusion.

The transport mechanisms are coupled with each other and depend on the membrane water content. As water is known to play the role of transport medium for proton [65], water dynamics and its relationship with the membrane structure are important parameters to study. In this work, pulsed-field gradient nuclear magnetic resonance (PFGNMR) is used to probe the water-self diffusion in sPEEK membranes at micrometric scale. This gives information on possible evolution of the water diffusion coefficient (Ds) induced by structural changes, as observed in the literature[18,66]. Since the water self-diffusion coefficient in a membrane is lower than in bulk water due to the tortuosity of the diffusion path any microstructure evolution can eventually induce a variation in this value[67].

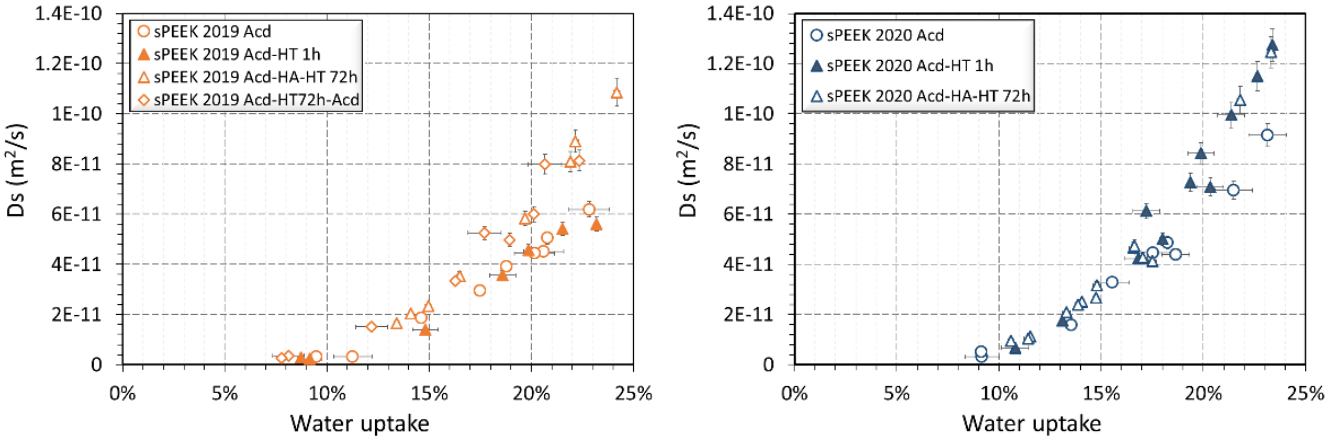

Figure 7. Water self-diffusion coefficient as a function of water uptake in sPEEK membranes from the 2019 batch (**Left**) and 2020 batch (**Right**).

Figure 7 shows the impact of the membrane pretreatments on the water self-diffusion coefficient Ds plotted as a function of the membrane water uptake. For water uptakes below 7 wt.%, none of the membranes show measurable water self-diffusion coefficient. Above 7 wt.%, the water self-diffusion coefficient of all membranes increases as expected with water uptake. However, significant differences between the pretreatments seem to occur above 14-15 wt.%: below these values, the microstructure modifications induced by the pretreatments, if any, have no impact on the water self-diffusion coefficient.

Membranes from the 2019 batch show similar behavior after acidification only (1st pretreatment: Acd) and acidification followed by a one-hour hydrothermal step in liquid water at 80°C (2nd pretreatment: Acd-HT 1h). However, this is not the case with membranes from the 2020 batch, which show a significant increase of the water self-diffusion coefficient at high water uptake when the hydrothermal step is applied.

Adding a hydro alcoholic stage and increasing the duration of the hydrothermal step does not improve further Ds in the 2020 batch membranes (4th pretreatment: Acd-HA-HT 72h), as illustrated in **Figure 7** (right). Again, the 2019 batch membranes behave differently, with a much more significant impact of both the hydro alcoholic stage and the longer hydrothermal

step, as shown in **Figure 7** (left). Finally, it must also be noted that water self-diffusion coefficients measured in sPEEK membranes are always much lower than the values usually encountered in PFSA membranes (of the order of 5 10^{-10} to 6 10^{-10} m²/s at high hydration level[27,63,68,69]), although the membrane ionic conductivity remains comparable (**Figure 6**, left). This last observation can be explained qualitatively by considering the spatial scales associated with these two measurements as well as the chemical nature of the two polymers. As the diffusion coefficient is measured by the NMR method over an observation time of a few milliseconds, the associated spatial scale is on the order of $\sim 1\,\mu m$. At this scale, the hydrophobic type interactions in PFSA are more favorable to faster diffusion than in the case of sPEEK where water wets the hydrocarbon backbone more easily. What the conductivity measurements show is that proton transport across the membrane must be favored by a better connectivity between conduction channels in sPEEK than in Nafion, so that proton transport is very efficient, despite a slower local water diffusion.

It is also interesting to note that the range of variation of the diffusion coefficient at maximum water content is of about 100% between the various pretreatments (with reference to the lowest value, i.e. 2019 Acd at $W_{water\ uptake}$~ 23 wt%) while the proton conductivity is multiplied by a factor of ~ 3 for the same samples (in water-saturated membranes). The expected structural modifications induced by the pretreatments do not have the same impacts on the water dynamics depending on the spatial scale at which it is observed. The acceleration of the water dynamics observed at the micron scale, probed by PFGNMR, is less important than the one seen by the conductivity measurement, resulting from an average at the global scale of the membrane. This is noteworthy and should be the subject of further structural study.

3.5. Water sorption

Figure 8 (above) shows water uptakes of a 2020 Fumapem E730 membrane sample (4th pretreatment: Acd-HA-HT 72h) as a function of time, to illustrate its very slow sorption kinetics. As mentioned in section 2.4, the maximum time for each humidity step was set to either 10 hours or 40 hours, and **Figure 8** (top, left) shows that 10 hours do not seem sufficient to reach equilibrium (i.e., $\frac{m(t)}{m_\infty} \geq 99\%$); 40 hours allowed to get closer (**Figure 8**, above right), while still being insufficient to reach 99% of the assumed equilibrium sample weight, except for the first RH step. Nevertheless, the impact of a 10 hours or 40 hours maximum equilibrium time on the assessed value of m_∞ is very low, as illustrated by the shape of the sorption isotherms in **Figure 8** (below).

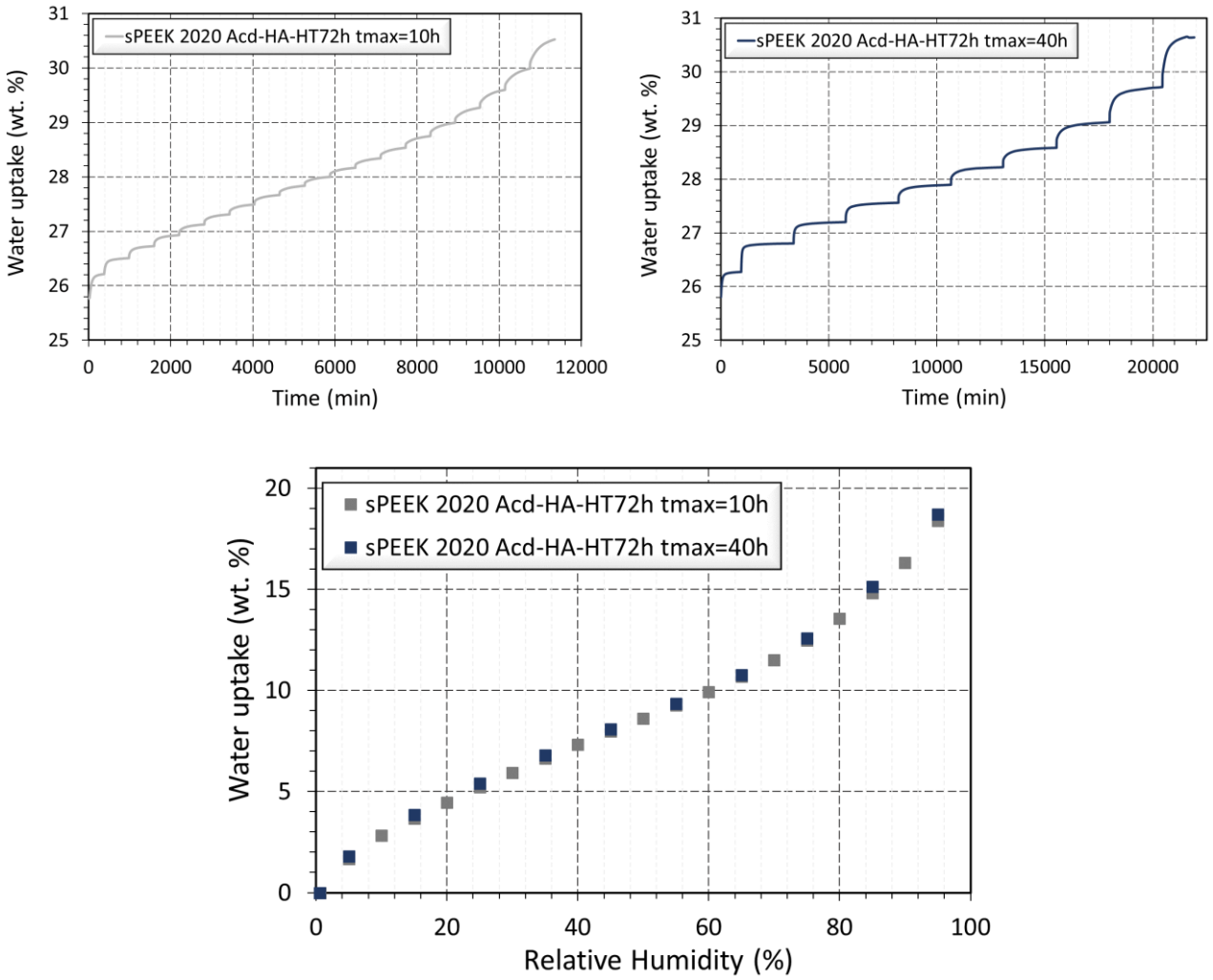

Figure 8. Above: water uptake versus time of sPEEK 2020 Acd-HA-HT 72h membrane from 5% to 95% RH. Measurements were made at 30°C and for maximum equilibrium times of 10 hours (left) and 40 hours (right). **Below**: comparison of sPEEK 2020 Acd-HA-HT 72h sorption isotherms determined with a 10-hours maximum equilibrium time and with a 40-hours equilibrium time.

Such a small and negligible impact of a 10 hours or 40 hours maximum equilibrium time was observed with the 3 other pretreatments, independently of the membrane batch (2019 or 2020). Therefore, **Figure 9** showing the water sorption isotherms of all sPEEK membranes was plotted using data from both protocols: the small error bars confirm the very good reproducibility of the measurements, as long as they are performed using the same sample.

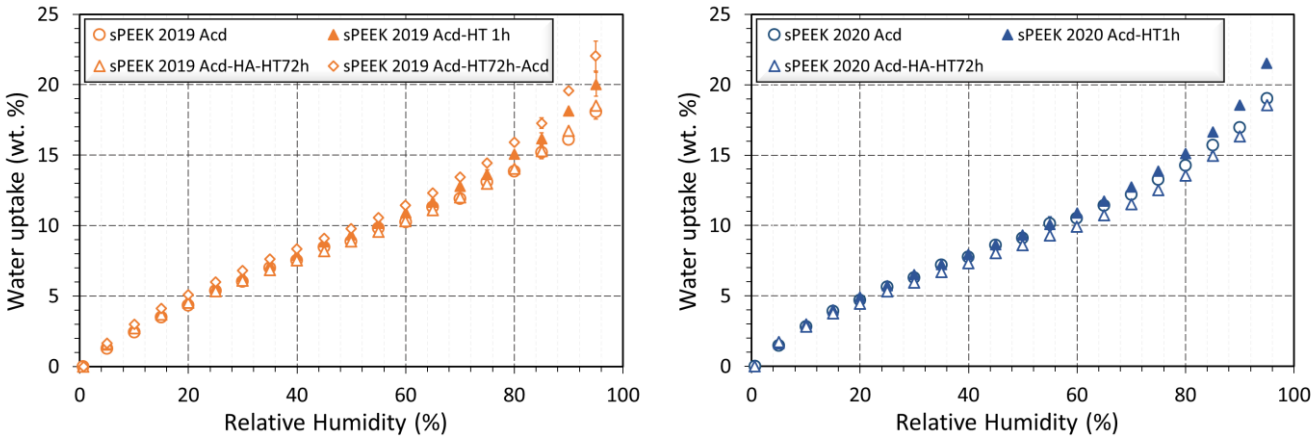

Figure 9. Water sorption isotherms as functions of air RH in sPEEK membranes from the 2019 batch (**Left**) and 2020 batch (**Right**). Data appearing on the graphs correspond to the average values measured using a maximum sorption time per humidity step of 10 hours and 40 hours.

Figure 9 illustrates the impact of the membrane pretreatments on water sorption isotherms. Some differences can be observed between them, mostly at the highest humidity contents (above 70% RH). The most influential pretreatments regarding water uptake appear to be the third (sPEEK 2019 Acd-HT 72h-Acd) in the case of the 2019 batch and the second (sPEEK 2020 Acd-HT 1h) in the case of the 2020 batch. In both cases the differences are more pronounced at high humidity. Surprisingly, the fourth pretreatment (sPEEK 2020 Acd-HA-HT 72h) leads to a significant decrease of water uptake compared to acidification only (sPEEK 2020 Acd) with membranes from the 2020 batch.

For the time being, one can see that the results are not fully consistent with those of water diffusion, FC performance and membrane conductivity. Indeed, the membrane sample from the 2020 batch submitted to the fourth pretreatment (sPEEK 2020 Acd-HA-HT 72h) seems to adsorb less water than the other samples despite a better water self-diffusion coefficient (**Figure 7**), good membrane ionic conductivity, low high frequency resistance, and excellent FC performance (**Figure 5** and **Figure 6**).

4. Discussion

Fumapem E730 sPEEK membrane pretreatments have a huge impact on FC performance, as shown in section 3.3: in the best case, i.e. fourth pretreatment consisting in acidification, hydro-alcoholic and hydrothermal steps (sPEEK 2020 Acd-HA-HT 72h - see section 2.3) with a membrane from the 2020 batch, the voltage even exceeded values obtained with a MEA made with Nafion XL, a PFSA membrane of thickness similar to those of -as received- Fumapem E730. These good performances are explained by a low FC high frequency resistance, which is consistent with the good membrane conductivity (**Figure 6**), although it was measured in

different conditions (room temperature, after soaking the samples in water) from those of FC operation (70°C, and 80% RH inlet gases).

In addition, it appeared that -contrary to the others- this fourth pretreatment led to a significant membrane thinning of about 47% (see section 3.1). To estimate the contribution of this thinning (*vs*. as received 30 µm thick sPEEK membranes) to the FC performance, one can consider two extreme cases, keeping in mind that the high frequency resistance is normally the sum of the membrane ionic resistance $R_{membrane}$ and all interfacial resistances appearing in a single cell, i.e. $R_{hf} = R_{membrane} + R_{interfaces}$:

- First, assuming negligible interfacial resistances (i.e. $R_{hf} = R_{membrane}$), a 47 mΩ cm^{-2} R_{hf} (**Figure 6**) obtained with a 17 µm membrane (section 3.1 and **Table 2**) corresponds to an equivalent sPEEK ionic conductivity of 36 mS cm^{-1}, which is far from what we measured in ambient conditions; with that same -equivalent- ionic conductivity, a 30 µm membrane would have an ionic resistance of about 83 mΩ cm^{-2}. However, such a 36 mΩ cm^{-2}, or 76%, increase of $R_{membrane}$ would lead to supplementary voltage losses of the order of only 18 mV at 0.5 A cm^{-2}, and 36 mV at 1.0 A cm^{-2} (vs. a FC voltage equal to 0.681 V and 0.631 V, respectively).
- On the other hand, assuming a membrane conductivity of 80 mS cm^{-1} (as measured in ambient conditions, see **Figure 6**), the ionic resistance of a 17 µm membrane is equal to about 21 mΩ cm^{-2}, so that interfacial resistances should be of the order of $R_{interfaces}$ = 26 mΩ cm^{-2} to reach 47 mΩ cm^{-2}, i.e. the estimated value of $R_{hf} = R_{membrane} + R_{interfaces}$ in **Figure 6**; in that case, increasing the membrane thickness to 30 µm by keeping both the interfacial resistances and the membrane conductivity constant would yield a high frequency resistance R_{hf} of about 64 mΩ cm^{-2}. Such a 17 mΩ cm^{-2} increase of R_{hf} due to a thicker membrane would lead to supplementary voltage losses of the order of 8 mV at 0.5 A cm^{-2} and 17 mV at 1.0 A cm^{-2} (vs. a FC voltage equal to 0.681 V and 0.631 V, respectively).

As one can see from these estimations, the lower thickness of the sPEEK membrane subjected to the fourth pretreatment (sPEEK 2020 Acd-HA-HT 72h) has a limited impact (no more than a few tenths of mV at 1.0 A cm^{-2}) on the fuel cell voltage, so that the main reason for its good performance is most probably its better ionic conductivity. As a complement, one can add that the estimation of $R_{interfaces}$ = 26 mΩ cm^{-2} in our second scenario (giving the lowest impact of the membrane thickness) is consistent with $R_{interfaces}$ = 25 mΩ cm^{-2}, as estimated in **Figure 6**. This shows that the membrane actual conductivity in real FC operating conditions is probably quite close to its measured value of 80 mS cm^{-1}.

sPEEK pretreatments also have a significant impact on water self-diffusion coefficient, the highest values being measured with the samples subjected to the fourth pretreatment, i.e. those giving the best FC performances (**Figure *7***). However, it must be noted that regardless of the applied pretreatment, the impacts are the strongest at high water uptake: i.e. above 20 wt.%, which corresponds according to the sorption isotherms to a gas relative humidity of 90% or more. These conditions are also close to those encountered by the membrane in the FC since the gas inlet RH was set to 80%; and they tend to humidify along the flow field plates.

Finally, the only inconsistency in the results lies in the water sorption isotherms: the water uptake measured after applying the fourth pretreatment to a membrane sample from the 2020 batch appeared to be lower than with the other pretreatments; this is in contradiction with the better -vs. other pretreatments- FC performance, ionic conductivity, and water self-diffusion coefficient discussed previously. Indeed, those parameters are -at least in theory- highly dependent on water uptake. To illustrate this point, and more specifically the link between the water self-diffusion coefficient and the FC performance, we estimated its values starting from the sorption curves, at 80% RH (i.e. FC inlet conditions) and 95% RH considering that gases tend to humidify along the flow field plates. These values were then compared to the FC high frequency resistances at 0.5 and 1.0 $A.cm^{-2}$ for each membrane (**Figure *10***, left). Like in the case of the proton conductivity (**Figure 6**), one can observe a good correlation between the water self-diffusion coefficient and the FC R_{hf}: overall, a lower water self-diffusion coefficient corresponds to a higher FC high frequency resistance, this in both 80% and 95% RH conditions. Similarly, a higher water self-diffusion coefficient also corresponds to a higher membrane ionic conductivity (**Figure *10***, right).

However, one can also observe that sPEEK membranes from the 2020 batch subjected to the fourth pretreatment (Acd-HA-HT 72h) do not follow these trends, with low R_{hf} (**Figure *10***, left) and high ionic conductivity (**Figure *10***, right) despite relatively low values of Ds. There may be several explanations to those different behavior:

- Regarding FC performance (i.e. FC R_{hf} in **Figure *10***, left and FC voltage in **Figure 5**), it should be borne in mind that the operating conditions are quite different from those under which the water self-diffusion coefficient was measured. The temperature was higher (70°C vs. 24°C) and in addition, one does not fully master the humidity condition at the membrane/electrode interfaces: with high gas inlet RH (80%) and low stoichiometries (1.5 for both oxygen and hydrogen), water activity is probably very close to one over a large part of the flow field plates.
- Regarding the membrane ionic conductivity, the temperature argument cannot be put forward since it was similar in both cases. However, this behavior could be explained

by a more confined structure at the micro scale -impacting the value of Ds - and a more structured configuration at higher scale inducing higher conductivity[70].

Although there can be no clear conclusion to this discussion without further results, it allows us to highlight the important role of water diffusion in sPEEK membranes, in terms of FC applications at least. Indeed, water self-diffusion coefficients being much lower in sPEEK membranes than in PFSA membranes (≈10^{-10} vs. 5 10^{-10} to 6 10^{-10} m²/s at high hydration level[27,63,68,69]), one may expect less interesting performances in low humidity conditions (and as a consequence, high temperature conditions) and/or with higher gas stoichiometry (when for instance the FC is fed with air) than in our case, i.e. a FC fed with 80% RH pure oxygen and hydrogen.

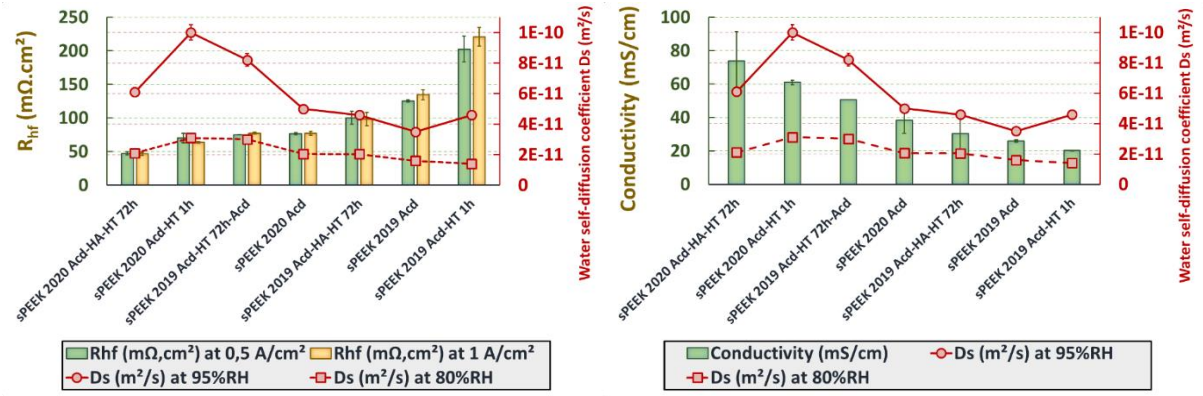

Figure 10. Left: high frequency resistance and membrane water self-diffusion coefficient at room temperature and 80% or 95% RH vs. sPEEK pretreatments. **Right:** conductivity and membrane water self-diffusion coefficient at room temperature and 80% or 95% RH vs. sPEEK pretreatments.

The intimate connections between water sorption, water diffusion and proton transport properties are by nature difficult to interpret because they are subject to multiple dependencies. In particular, the relationships between polymer microstructure and transport properties will need to be probed in more detail by scattering experiments such as SAXS and SANS. The modifications of nano-structuration induced by the different pre-treatments could then allow to better understand and rationalize the impact of the pretreatments on the functional properties of the polymer. The data set could also contribute to the understanding of the differences observed between the two batches of membranes studied. As a side note, let us emphasize that such differences in behavior and properties between the 2019 and 2020 sPEEK batches also highlight the importance of the ionomer micro/nanostructure, since the ionomer chemical formulation remains unchanged in both cases.

5. Conclusions

We examined the impact of pretreatments applied on sulfonated Poly(Ether Ether Ketone) (sPEEK) membranes in terms of functional properties and fuel cell performance. This work

was carried out using two different batches of Fumapem E730 from Fumatech, acquired in 2019 and in 2020.

Overall, four different protocols were used. The simplest protocol consisted in soaking the membrane in an acid solution at 80°C followed by a rinsing step in water at room temperature and a drying step. Then, in addition to this acidification step, hydrothermal treatments in water at high temperature were applied: either one hour as recommended by the membrane manufacturer, or 72 hours following recent results of the literature showing an optimum sPEEK nano-structuration in this case [18]. Finally, the fourth protocol also included a hydro-alcoholic step, because of its expected effects on the ionomer nanostructure[66].

The results show that pretreatments have a huge impact on Fumapem E730 membranes performance when used in fuel cells, as well as on other functional properties such as ionic conductivity, water self-diffusion coefficient and water sorption. The best performances were obtained with the fourth pretreatment, consisting in acidification, hydro-alcoholic and hydrothermal steps and with a membrane from the 2020 batch. In this case, the FC polarization curves even exceeded those obtained with a MEA made -for comparison purpose- using a Nafion XL PFSA membrane. In line with these results, sPEEK membranes of the 2020 batch subjected to this protocol also showed high water self-diffusion coefficient and ionic conductivity but surprisingly, a slightly lower water uptake than the other samples.

In further studies, the relationships between polymer microstructure and transport properties will be probed in more detail by scattering experiments (SAXS and SANS) to better interpret the connections between water sorption, water diffusion and proton transport properties in nanostructured sPEEK membranes.

In addition, another perspective to this study will consist in durability tests carried out in varied operating conditions, including higher temperature.

Despite of these good results, providing functional membrane-electrodes assemblies using sPEEK membranes remains complicated due to the use of PFSA in the electrode as binder - in terms of adhesion and ionic resistance. In our case, the MEA could be assembled only by applying a thin PFSA overcoat on the gas diffusion electrodes before hot-pressing onto the membrane. It will therefore be necessary to optimize the fabrication process to mitigate the interface resistance associated with the PFSA overcoat.

6. References

[1] A. Saadi, M. Becherif, D. Hissel, H.S. Ramadan, Dynamic modeling and experimental analysis of PEMFCs: A comparative study, Int. J. Hydrog. Energy. 42 (2017) 1544–1557. https://doi.org/10.1016/j.ijhydene.2016.07.180.

[2] H.P. Dhar, On solid polymer fuel cells, J. Electroanal. Chem. 357 (1993) 237–250. https://doi.org/10.1016/0022-0728(93)80382-R.

[3] Y.I. Cho, Y. Jeon, Y.-G. Shul, Enhancement of the electrochemical membrane electrode assembly in proton exchange membrane fuel cells through direct microwave treatment, J. Power Sources. 263 (2014) 46–51. https://doi.org/10.1016/j.jpowsour.2014.04.016.

[4] L. Maldonado, J.-C. Perrin, J. Dillet, O. Lottin, Characterization of polymer electrolyte Nafion membranes: Influence of temperature, heat treatment and drying protocol on sorption and transport properties, J. Membr. Sci. 389 (2012) 43–56. https://doi.org/10.1016/j.memsci.2011.10.014.

[5] M. Robert, Impact of degradation and aging on properties of PFSA membranes for fuel cells, Université de Lorraine, 2021. http://www.theses.fr/2021LORR0004.

[6] K.A. Mauritz, R.B. Moore, State of Understanding of Nafion, Chem. Rev. 104 (2004) 4535–4586. https://doi.org/10.1021/cr0207123.

[7] S.J. Paddison, R. Paul, The nature of proton transport in fully hydrated Nafion®, Phys. Chem. Chem. Phys. 4 (2002) 1158–1163. https://doi.org/10.1039/b109792j.

[8] H. Zhang, X. Li, C. Zhao, T. Fu, Y. Shi, H. Na, Composite membranes based on highly sulfonated PEEK and PBI: Morphology characteristics and performance, J. Membr. Sci. 308 (2008) 66–74. https://doi.org/10.1016/j.memsci.2007.09.045.

[9] M.-S. Jun, Y.-W. Choi, J.-D. Kim, Solvent casting effects of sulfonated poly(ether ether ketone) for Polymer electrolyte membrane fuel cell, J. Membr. Sci. 396 (2012) 32–37. https://doi.org/10.1016/j.memsci.2011.12.008.

[10] S. Kaliaguine, S.D. Mikhailenko, K.P. Wang, P. Xing, G. Robertson, M. Guiver, Properties of SPEEK based PEMs for fuel cell application, Catal. Today. 82 (2003) 213–222. https://doi.org/10.1016/S0920-5861(03)00235-9.

[11] K.N.T. Do, D. Kim, Comparison of homogeneously and heterogeneously sulfonated polyetheretherketone membranes in preparation, properties and cell performance, J. Power Sources. 185 (2008) 63–69. https://doi.org/10.1016/j.jpowsour.2008.06.087.

[12] V. Elumalai, C.K. Kavya Sravanthi, D. Sangeetha, Synthesis characterization and performance evaluation of tungstic acid functionalized SBA-15/SPEEK composite membrane for proton exchange membrane fuel cell, Appl. Nanosci. 9 (2019) 1163–1172. https://doi.org/10.1007/s13204-019-01005-5.

[13] N. Huynh, J.P.C. Fernandes, P.A. Bayle, M. Bardet, E. Espuche, J. Dillet, J.-C. Perrin, A. El Kaddouri, O. Lottin, V.H. Mareau, H. Mendil-Jakani, L. Gonon, Sol-gel route: An original strategy to chemically stabilize proton exchange membranes for fuel cell, J. Power Sources. 462 (2020) 228164. https://doi.org/10.1016/j.jpowsour.2020.228164.

[14] D.M. Xing, B.L. Yi, F.Q. Liu, Y.Z. Fu, H.M. Zhang, Characterization of Sulfonated Poly(Ether Ether Ketone)/Polytetrafluoroethylene Composite Membranes for Fuel Cell Applications, Fuel Cells. 5 (2005) 406–411. https://doi.org/10.1002/fuce.200500089.

[15] M.J. Parnian, S. Rowshanzamir, A.K. Prasad, S.G. Advani, High durability sulfonated poly (ether ether ketone)-ceria nanocomposite membranes for proton exchange membrane fuel cell applications, J. Membr. Sci. 556 (2018) 12–22. https://doi.org/10.1016/j.memsci.2018.03.083.

[16] H. Hou, M.L. Di Vona, P. Knauth, Durability of Sulfonated Aromatic Polymers for Proton-Exchange-Membrane Fuel Cells, ChemSusChem. 4 (2011) 1526–1536. https://doi.org/10.1002/cssc.201000415.

[17] H. Mendil-Jakani, I. Zamanillo Lopez, P.M. Legrand, V.H. Mareau, L. Gonon, A new interpretation of SAXS peaks in sulfonated poly(ether ether ketone) (sPEEK) membranes for fuel cells, Phys Chem Chem Phys. 16 (2014) 11243–11250. https://doi.org/10.1039/C4CP00710G.

[18] H. Mendil-Jakani, I. Zamanillo López, V.H. Mareau, L. Gonon, Optimization of hydrophilic/hydrophobic phase separation in sPEEK membranes by hydrothermal treatments, Phys. Chem. Chem. Phys. 19 (2017) 16013–16022. https://doi.org/10.1039/C7CP00087A.
[19] Legrand, P.M., Gonon, L., Mareau, V.H., Morin, A, Méthode de traitement d'une membrane conductrice protonique permettant d'améliorer ses propriétés., FR1250476, 2012.
[20] P. Xing, G.P. Robertson, M.D. Guiver, S.D. Mikhailenko, K. Wang, S. Kaliaguine, Synthesis and characterization of sulfonated poly(ether ether ketone) for proton exchange membranes, J. Membr. Sci. 229 (2004) 95–106. https://doi.org/10.1016/j.memsci.2003.09.019.
[21] M.J. Parnian, S. Rowshanzamir, F. Gashoul, Comprehensive investigation of physicochemical and electrochemical properties of sulfonated poly (ether ether ketone) membranes with different degrees of sulfonation for proton exchange membrane fuel cell applications, Energy. 125 (2017) 614–628. https://doi.org/10.1016/j.energy.2017.02.143.
[22] H.-Y. Jung, J.W. Kim, Role of the glass transition temperature of Nafion 117 membrane in the preparation of the membrane electrode assembly in a direct methanol fuel cell (DMFC), Int. J. Hydrog. Energy. 37 (2012) 12580–12585. https://doi.org/10.1016/j.ijhydene.2012.05.121.
[23] M. Divona, Z. Ahmed, S. Bellitto, A. Lenci, E. Traversa, S. Licoccia, SPEEK-TiO2 nanocomposite hybrid proton conductive membranes via in situ mixed sol–gel process, J. Membr. Sci. 296 (2007) 156–161. https://doi.org/10.1016/j.memsci.2007.03.037.
[24] M. Kumari, H.S. Sodaye, R.C. Bindal, Effect of phosphotungstic acid blending on properties of sulfonated poly(ether ether ketone)-poly(ethylene glycol) crosslinked membranes, J. Appl. Polym. Sci. 135 (2018) 46667. https://doi.org/10.1002/app.46667.
[25] P.M. Legrand, A. Morin, V.H. Mareau, L. Gonon, Impact of gas stoichiometry on water management and fuel cell performance of a sulfonated Poly(Ether Ether Ketone) membrane, J. Power Sources. 206 (2012) 161–170. https://doi.org/10.1016/j.jpowsour.2012.01.102.
[26] G. Gebel, Structure of Membranes for Fuel Cells: SANS and SAXS Analyses of Sulfonated PEEK Membranes and Solutions, Macromolecules. 46 (2013) 6057–6066. https://doi.org/10.1021/ma400314c.
[27] K.D. Kreuer, On the development of proton conducting polymer membranes for hydrogen and methanol fuel cells, J. Membr. Sci. 185 (2001) 29–39. https://doi.org/10.1016/S0376-7388(00)00632-3.
[28] B. Yang, A. Manthiram, Comparison of the small angle X-ray scattering study of sulfonated poly(etheretherketone) and Nafion membranes for direct methanol fuel cells, J. Power Sources. 153 (2006) 29–35. https://doi.org/10.1016/j.jpowsour.2005.03.185.
[29] G. Portale, A. Carbone, A. Martinelli, E. Passalacqua, Microstructure, state of water and proton conductivity of sulfonated poly(ether ether ketone), Solid State Ion. 252 (2013) 62–67. https://doi.org/10.1016/j.ssi.2013.08.031.
[30] G. Gebel, P. Aldebert, M. Pineri, Swelling study of perfluorosulphonated ionomer membranes, Polymer. 34 (1993) 333–339. https://doi.org/10.1016/0032-3861(93)90086-P.
[31] K.S. Santhosh Kumar, K.P. Vijayalakshmi, S. Sivanath, T. Jayalatha, S. Mohanty, M. Shaneeth, Interaction of nafion ionomers toward various solvents, J. Appl. Polym. Sci. 128 (2013) 3710–3719. https://doi.org/10.1002/app.38421.
[32] P. Pei, Z. Wu, Y. Li, X. Jia, D. Chen, S. Huang, Improved methods to measure hydrogen crossover current in proton exchange membrane fuel cell, Appl. Energy. 215 (2018) 338–347. https://doi.org/10.1016/j.apenergy.2018.02.002.
[33] M. Breitwieser, M. Klingele, S. Vierrath, R. Zengerle, S. Thiele, Tailoring the Membrane-Electrode Interface in PEM Fuel Cells: A Review and Perspective on Novel Engineering Approaches, Adv. Energy Mater. 8 (2018) 1701257. https://doi.org/10.1002/aenm.201701257.

[34] S. Sambandam, V. Ramani, Effect of cathode binder IEC on kinetic and transport losses in all-SPEEK MEAs, Electrochimica Acta. 53 (2008) 6328–6336. https://doi.org/10.1016/j.electacta.2008.04.012.
[35] E.B. Easton, T.D. Astill, S. Holdcroft, Properties of Gas Diffusion Electrodes Containing Sulfonated Poly(ether ether ketone), J. Electrochem. Soc. 152 (2005) A752. https://doi.org/10.1149/1.1864412.
[36] H.-Y. Jung, J.-K. Park, Long-term performance of DMFC based on the blend membrane of sulfonated poly(ether ether ketone) and poly(vinylidene fluoride), Int. J. Hydrog. Energy. 34 (2009) 3915–3921. https://doi.org/10.1016/j.ijhydene.2009.02.065.
[37] K.B. Wiles, C.M. de Diego, J. de Abajo, J.E. McGrath, Directly copolymerized partially fluorinated disulfonated poly(arylene ether sulfone) random copolymers for PEM fuel cell systems: Synthesis, fabrication and characterization of membranes and membrane–electrode assemblies for fuel cell applications, J. Membr. Sci. 294 (2007) 22–29. https://doi.org/10.1016/j.memsci.2007.01.036.
[38] M.-J. Choo, K.-H. Oh, H. Park, J.-K. Park, New cross-linked interfacial layer on hydrocarbon membrane to improve long-term stability of polymer electrolyte fuel cells, Electrochimica Acta. 92 (2013) 285–290. https://doi.org/10.1016/j.electacta.2013.01.038.
[39] D.M. Yu, T.-H. Kim, J.Y. Lee, S. Yoon, Y.T. Hong, Thin bonding layer using sulfonated poly(arylene ether sulfone)/PVdF blends for hydrocarbon-based membrane electrode assemblies, Electrochimica Acta. 173 (2015) 268–275. https://doi.org/10.1016/j.electacta.2015.05.031.
[40] S.-W. Nam, D.M. Yu, T.-H. Kim, J.Y. Lee, S.Y. Nam, Y.T. Hong, Synthesis and properties of bonding layer containing flexible and fluorinated moieties for hydrocarbon-based membrane electrode assemblies, Int. J. Hydrog. Energy. 41 (2016) 10884–10895. https://doi.org/10.1016/j.ijhydene.2016.04.174.
[41] H.Y. Jeong, D.-S. Yang, J.H. Han, J.Y. Lee, S. So, D.H. Suh, S.K. Hong, Y.T. Hong, T.-H. Kim, Novel interfacial bonding layers with controlled gradient composition profile for hydrocarbon-based membrane electrode assemblies, J. Power Sources. 398 (2018) 1–8. https://doi.org/10.1016/j.jpowsour.2018.07.045.
[42] K. Oh, H.S. Kang, M. Choo, D. Jang, D. Lee, D.G. Lee, T. Kim, Y.T. Hong, J. Park, H. Kim, Interlocking Membrane/Catalyst Layer Interface for High Mechanical Robustness of Hydrocarbon-Membrane-Based Polymer Electrolyte Membrane Fuel Cells, Adv. Mater. 27 (2015) 2974–2980. https://doi.org/10.1002/adma.201500328.
[43] L. Gubler, H. Kuhn, T.J. Schmidt, G.G. Scherer, H.-P. Brack, K. Simbeck, Performance and Durability of Membrane Electrode Assemblies Based on Radiation-Grafted FEP-g-Polystyrene Membranes, Fuel Cells. 4 (2004) 196–207. https://doi.org/10.1002/fuce.200400019.
[44] J. Peron, Z. Shi, S. Holdcroft, Hydrocarbon proton conducting polymers for fuel cell catalyst layers, Energy Environ. Sci. 4 (2011) 1575. https://doi.org/10.1039/c0ee00638f.
[45] A. Ayad, J. Bouet, J.F. Fauvarque, Comparative study of protonic conducting polymers incorporated in the oxygen electrode of the PEMFC, J. Power Sources. 149 (2005) 66–71. https://doi.org/10.1016/j.jpowsour.2005.02.044.
[46] E. Moukheiber, Understanding of the structure of perfluorinated sulfonic membranes for fuel cell, UNIVERSITÉ DE GRENOBLE, 2011.
[47] M. Robert, A. El Kaddouri, J.-C. Perrin, K. Mozet, M. Daoudi, J. Dillet, J.-Y. Morel, S. André, O. Lottin, Effects of conjoint mechanical and chemical stress on perfluorosulfonic-acid membranes for fuel cells, J. Power Sources. 476 (2020) 228662. https://doi.org/10.1016/j.jpowsour.2020.228662.
[48] K.A. Page, K.M. Cable, R.B. Moore, Molecular Origins of the Thermal Transitions and Dynamic Mechanical Relaxations in Perfluorosulfonate Ionomers, Macromolecules. 38 (2005) 6472–6484. https://doi.org/10.1021/ma0503559.
[49] D.J. Kim, B.-N. Lee, S.Y. Nam, Characterization of highly sulfonated PEEK based membrane for the fuel cell application, Int. J. Hydrog. Energy. 42 (2017) 23768–23775. https://doi.org/10.1016/j.ijhydene.2017.04.082.

[50] M.-S. Jun, Y.-W. Choi, J.-D. Kim, Solvent casting effects of sulfonated poly(ether ether ketone) for Polymer electrolyte membrane fuel cell, J. Membr. Sci. 396 (2012) 32–37. https://doi.org/10.1016/j.memsci.2011.12.008.
[51] J. Crank, E.P.J. Crank, The Mathematics of Diffusion, Clarendon Press, 1979.
[52] E.O. Stejskal, J.E. Tanner, Spin Diffusion Measurements: Spin Echoes in the Presence of a Time-Dependent Field Gradient, J. Chem. Phys. 42 (1965) 288–292. https://doi.org/10.1063/1.1695690.
[53] I. Pivac, B. Šimić, F. Barbir, Experimental diagnostics and modeling of inductive phenomena at low frequencies in impedance spectra of proton exchange membrane fuel cells, J. Power Sources. 365 (2017) 240–248. https://doi.org/10.1016/j.jpowsour.2017.08.087.
[54] J. Mainka, Local impedance in H2/air Proton Exchange Membrane Fuel Cells (PEMFC) Theoretical and experimental investigations, Université Henri Poincaré - Nancy 1, 2011. http://docnum.univ-lorraine.fr/public/SCD_T_2011_0042_MAINKA.pdf.
[55] E. Antolini, L. Giorgi, A. Pozio, E. Passalacqua, Influence of Nafion loading in the catalyst layer of gas-diffusion electrodes for PEFC, J. Power Sources. 77 (1999) 136–142. https://doi.org/10.1016/S0378-7753(98)00186-4.
[56] S. Touhami, L. Dubau, J. Mainka, J. Dillet, M. Chatenet, O. Lottin, Anode aging in polymer electrolyte membrane fuel Cells I: Anode monitoring by ElectroChemical impedance spectroscopy, J. Power Sources. 481 (2021) 228908. https://doi.org/10.1016/j.jpowsour.2020.228908.
[57] T. Gaumont, G. Maranzana, O. Lottin, J. Dillet, S. Didierjean, J. Pauchet, L. Guétaz, Measurement of protonic resistance of catalyst layers as a tool for degradation monitoring, Int. J. Hydrog. Energy. 42 (2017) 1800–1812. https://doi.org/10.1016/j.ijhydene.2016.10.035.
[58] S. Abbou, J. Dillet, G. Maranzana, S. Didierjean, O. Lottin, Local potential evolutions during proton exchange membrane fuel cell operation with dead-ended anode – Part I: Impact of water diffusion and nitrogen crossover, J. Power Sources. 340 (2017) 337–346. https://doi.org/10.1016/j.jpowsour.2016.11.079.
[59] A. Lamibrac, G. Maranzana, J. Dillet, O. Lottin, S. Didierjean, J. Durst, L. Dubau, F. Maillard, M. Chatenet, Local Degradations Resulting from Repeated Start-ups and Shut-downs in Proton Exchange Membrane Fuel Cell (PEMFC), Energy Procedia. 29 (2012) 318–324. https://doi.org/10.1016/j.egypro.2012.09.038.
[60] P. Legrand, Influence des conditions de fonctionnement de la pile à combustible sur les performances du dispositif et la durabilité de la membrane, Université de Grenoble, 2012. https://tel.archives-ouvertes.fr/tel-00767130/document.
[61] S. He, Y. Lin, H. Ma, H. Jia, X. Liu, J. Lin, Preparation of sulfonated poly(ether ether ketone) (SPEEK) membrane using ethanol/water mixed solvent, Mater. Lett. 169 (2016) 69–72. https://doi.org/10.1016/j.matlet.2016.01.099.
[62] X. Liu, S. He, S. Liu, H. Jia, L. Chen, B. Zhang, L. Zhang, J. Lin, The roles of solvent type and amount of residual solvent on determining the structure and performance of sulfonated poly(ether ether ketone) proton exchange membranes, J. Membr. Sci. 523 (2017) 163–172. https://doi.org/10.1016/j.memsci.2016.10.007.
[63] M. Robert, A. El Kaddouri, M. Crouillere, J.-C. Perrin, L. Dubau, F. Dubelley, K. Mozet, M. Daoudi, J. Dillet, J.-Y. Morel, S. Leclerc, O. Lottin, A chemical-mechanical ex-situ aging of perfluorosulfonic-acid membranes for fuel cells: Impact on the structure and the functional properties, J. Power Sources. 520 (2022) 230911. https://doi.org/10.1016/j.jpowsour.2021.230911.
[64] M. Robert, A. El Kaddouri, J.-C. Perrin, K. Mozet, J. Dillet, J.-Y. Morel, O. Lottin, The Impact of Chemical-Mechanical Ex Situ Aging on PFSA Membranes for Fuel Cells, Membranes. 11 (2021) 366. https://doi.org/10.3390/membranes11050366.
[65] K.-D. Kreuer, S.J. Paddison, E. Spohr, M. Schuster, Transport in Proton Conductors for Fuel-Cell Applications: Simulations, Elementary Reactions, and Phenomenology, Chem. Rev. 104 (2004) 4637–4678. https://doi.org/10.1021/cr020715f.

[66] C.A. Kawaguti, K. Dahmouche, A. de S. Gomes, Nanostructure and properties of proton-conducting sulfonated poly(ether ether ketone) (SPEEK) and zirconia-SPEEK hybrid membranes for direct alcohol fuel cells: effect of the nature of swelling solvent and incorporation of heteropolyacid: Proton-conducting SPEEK and zirconia-SPEEK membranes, Polym. Int. 61 (2012) 82–92. https://doi.org/10.1002/pi.3151.
[67] A. Guillermo, G. Gebel, H. Mendil-Jakani, E. Pinton, NMR and Pulsed Field Gradient NMR Approach of Water Sorption Properties in Nafion at Low Temperature, J. Phys. Chem. B. 113 (2009) 6710–6717. https://doi.org/10.1021/jp8110452.
[68] M. Robert, A.E. Kaddouri, J.-C. Perrin, S. Leclerc, O. Lottin, Towards a NMR-Based Method for Characterizing the Degradation of Nafion XL Membranes for PEMFC, J. Electrochem. Soc. 165 (2018) F3209–F3216. https://doi.org/10.1149/2.0231806jes.
[69] M. Robert, A. El Kaddouri, J.-C. Perrin, J. Raya, O. Lottin, Time-resolved monitoring of composite Nafion™ XL membrane degradation induced by Fenton's reaction, J. Membr. Sci. 621 (2021) 118977. https://doi.org/10.1016/j.memsci.2020.118977.
[70] J.-C. Perrin, Etude expérimentale multi-échelles de la dynamique de l'eau dans les membranes ionomères utilisées en pile à combustible, Université Joseph Fourier - Grenoble I, 2006.